Kinetics of Oxygen Consumption and Light-induced Changes of Nucleotides in Solitary Rod Photoreceptors

SERGE POITRY,* MARCOS TSACOPOULOS,* ALAN FEIN,‡ and M. CARTER CORNWALL§

From the *Experimental Ophthalmology Laboratory and Department of Physiology, University of Geneva School of Medicine, 1211 Geneva 4, Switzerland; ‡Department of Physiology, University of Connecticut Health Center, Farmington, Connecticut 06032; and §Department of Physiology, Boston University School of Medicine, Boston, Massachusetts 02118

ABSTRACT We made simultaneous measurements of light-induced changes in the rate of oxygen consumption (QO_2) and transmembrane current of single salamander rod photoreceptors. Since the change of PO_2 was suppressed by 2 mM Amytal, an inhibitor of mitochondrial respiration, we conclude that it is mitochondrial in origin. To identify the cause of the change of QO_2, we measured, in batches of rods, the concentrations of ATP and phosphocreatine (PCr). After 3 min of illumination, when the QO_2 had decreased ~25%, ATP levels did not change significantly; in contrast, the amount of PCr had decreased ~40%. We conclude that either the light-induced decrease of QO_2 is not caused by an increase in [ATP] or [PCr], or that the light-induced change of [PCr] is highly heterogenous in the rod cell. Key words: metabolism • ATP • retina • phototransduction • creatine phosphate

INTRODUCTION

A fundamental problem of cellular neurobiology is how neurons regulate their metabolism to provide energy for cellular work. For muscle and liver cells, most textbooks state that the primary mechanism by which oxidative metabolism is regulated is by the availability of ADP as the phosphate acceptor of respiration (for example see, Lehninger, 1982; Darnell et al., 1986). However, despite the bulk of experimental data, there is little direct evidence that this is, in fact, how living cells in general and neurons in particular regulate their metabolism (McCormack and Denton, 1994). One of the major difficulties encountered in studying this regulation in the nervous system is the structural and functional heterogeneity of this system: the brain and the retina, for example, are made of several types of neurons and glial cells which may differ in their metabolic response to a particular stimulus or treatment. The goal of the experiments reported here was to test this assertion in a single identified neuron.

The rod photoreceptor is a highly compartmentalized cell (Fein and Szuts, 1982) and is described as being composed of an inner and an outer segment interconnected by a cilium. While the outer segment is specifically devoted to phototransduction (it contains the visual pigment and all the other molecules necessary for visual transduction), the inner segment, which ends with the synaptic terminal, comprises the nucleus and other organelles; in particular, the mitochondria which are packed within the region of the inner segment adjacent to the outer segment. The large number of mitochondria in rod photoreceptors suggests that mitochondrial oxidative metabolism is necessary to sustain rod function, and this is supported by electrical recordings in the isolated retina where the rod response to light is suppressed by anoxia (Ames et al., 1992). We report here experiments in which we measured O_2 consumption and nucleotide levels on isolated rod photoreceptors, under closely matching experimental conditions. We find that light causes an overall decrease in O_2 consumption with a corresponding decrease in phosphocreatine (PCr)[1] level, which is precisely the opposite of what one would expect in a homogenous cell if the availability of ADP were regulating oxidative phosphorylation (see Discussion).

MATERIALS AND METHODS

Preparation

Larval tiger salamanders (*Ambystoma tigrinum*) were purchased from Charles Sullivan (Nashville, TN) and were kept in a tank filled with tap water maintained at 10°C under a 12-h dark, 12-h light cycle. Animals were dark-adapted for at least 3 h before their use. The dissection as well as all subsequent experimental manipulations were carried out under infrared illumination with the aid of infrared image converters (FJW Industries, Palatine, IL). The procedure for isolating photoreceptors was similar to that described previously (Cornwall et al., 1990). Briefly, after de-

Address correspondence to M. Carter Cornwall, Ph.D., Department of Physiology L714, Boston University School of Medicine, 80 E. Concord Street, Boston, Massachusetts 02118. Fax: 617-638-4273; E-mail: cornwall@bu.edu

[1] *Abbreviations used in this paper:* Ca_i, intracellular concentration of Ca; Na_i, intracellular concentration of Na; PCr, phosphocreatine; PO_2, partial pressure of oxygen; QO_2, rate of oxygen consumption.

J. GEN. PHYSIOL. © The Rockefeller University Press • 0022-1295/96/08/75/13 $2.00
Volume 108 August 1996 75–87

capitation of the animal, the eyes were removed and hemisected with a razor blade. Retinas were dissected from the eye cup and separated from the pigment epithelium with fine forceps and then placed in a small Petri dish filled with Ringer solution containing 1 mg/ml BSA. The retinas were then teased into small pieces and triturated by repeated passage through the tip of a Pasteur pipette. This cell suspension was finally transferred into a plastic tube and kept in darkness until used. At the beginning of an experiment, an aliquot (~1 ml) of this suspension was transferred to the recording chamber.

Chemicals

Unless otherwise indicated, all chemicals were purchased from Sigma Chemicals (Buchs, Switzerland).

The Ringer solution had the following composition: NaCl, 102 mM; KCl, 2.5 mM; $MgCl_2$, 1.6 mM; $CaCl_2$, 1 mM; glucose, 10 mM; HEPES, 10 mM; NaOH, 7 mM; pH 7.8. Solutions containing Amytal (Na-amobarbital; Fluka, Buchs, Switzerland) were prepared by its addition to the appropriate volume of Ringer solution. Measurements of ATP and PCr were made using a mixture of dry luciferin and luciferase (Lumit PM kit; Lumac B.V., Landgraaf, Netherlands) dissolved in a freshly prepared buffer solution containing: Mg acetate, 5 mM; EDTA, 2 mM; HEPES, 1 mM; NaOH, 50 mM; pH 7.4. The ADP used for the measurement of PCr was ADP-K from Boehringer (Mannheim, Germany) which initially contained ~0.2% ATP; this amount of ATP was decreased to ~0.02% using the procedure described by Passonneau and Lowry (1993). To eliminate possible traces of myokinase activity from the creatine kinase solution (see, Lust et al., 1981), P^1,P^5-Di(adenosine,5′) pentaphosphate (10^{-6} M) was added to that solution.

Light Stimulation

The light stimulator used for the physiological experiments is similar to that described in Cornwall et al. (1990). Light from a xenon arc was passed through a condensing lens and focused on an electromagnetic shutter. After passing through a 526-nm interference filter, a series of neutral density filters, and a diaphragm, the image of the filament was focused on the back plane of a 10× objective lens mounted in place of the condenser of a fixed stage compound microscope. When critically focused, a spot of uniform illumination 130 μm in diameter was located at the plane of the preparation. Its unattenuated intensity was 1.4×10^8 photons $\mu m^{-2}\ s^{-1}$. Unless otherwise indicated, the standard light stimulus consisted of 90 flashes, each 20 ms in duration, at a frequency of 0.5 Hz.

For the biochemical measurements of ATP and PCr a small number of isolated rods were collected into an aqueous droplet (see below). The light stimulator used for the biochemical measurements was the same as that described above except that after passage through the interference and neutral density filters, the light was collected and focused on to one end of a 5-mm diameter optical fiber cable. The other end of this cable was mounted on a micromanipulator so that it could be brought close to the droplet containing the rods. The intensity and wavelength of the beam emerging from the end of the fiber optic cable were adjusted to match those used in the electrophysiological experiments.

Electrophysiology

The method for recording the electrical activity of the rod photoreceptors was similar to that used by Cornwall et al. (1990) and is similar to techniques first described by Yau et al. (1981). An aliquot of the cell suspension was introduced into the recording chamber and allowed to settle to the bottom. The cells in the chamber could then be viewed under infrared illumination on a video monitor connected to an infrared sensitive video camera (TC2055 Ultricon; R.C.A., Lancaster, PA) fitted to the microscope. A rod photoreceptor, consisting of an intact inner and outer segment, was gently drawn into a tight-fitting glass pipette (see diagram in Fig. 1 *a*) which was connected to the head stage of a patch clamp amplifier (Model EPC7; List Electronic, Darmstadt, Germany) so as to monitor the transmembrane electrical current. The position of the cell in the current recording pipette was adjusted so that it was recessed ~10 μm from the tip. The tip of an O_2-sensitive microelectrode was then brought into the opening of the suction pipette to measure the PO_2 near the surface of the cell (see Fig. 1 *a*). This O_2-sensitive microelectrode was of the type described by Tsacopoulos et al. (1981). Its size at the tip was on the order of 2–5 μm, and the platinum filament was ~5 μm recessed. Typically, with −580 mV polarization, the current of the O_2-sensitive microelectrode was 70 pA in air-equilibrated Ringer solution. Unless otherwise indicated, the chamber was constantly perfused (~0.3 ml/min) with Ringer solution. All measurements were performed at room temperature (22°C).

Biochemistry

Retinal tissue containing rods, on which biochemical measurements were to be made, was prepared in the same way as for electrophysiological experiments. For these experiments, cells were introduced into the recording chamber and were then aspirated one by one into a glass pipette filled with Ringer solution. This pipette had an internal diameter two to three times as large as that of the tight-fitting pipettes used for electrophysiological measurements, and it was silanized. Typically, 30–70 cells, consisting of intact inner and outer segments, were collected in this way into the pipette. The pipette was then removed from the chamber and its whole contents (~30 μl) was expelled onto a small plastic sheet (~4 mm wide and 20 mm long). The droplet thus formed was either left to sit for 3 min in darkness or stimulated with light flashes. For stimulation, the end of the optical fiber was brought within 3–5 mm from the droplet. After stimulation (or dark control period), the plastic sheet was introduced into an Eppendorff tube and washed with 270 μl of DMSO to solubilize the cells (in preliminary measurements, we checked that nucleotide extraction in 90% DMSO is at least as efficient as in 10% trichloroacetic acid [see also Lundin et al., 1986], and it is easier to use). The content of the Eppendorff tube was then briefly vortexed and frozen in liquid nitrogen. Samples were then lyophilized to remove DMSO, resuspended in 70 μl of H_2O, and then frozen and stored in liquid nitrogen awaiting later analysis. Rod outer segments with no inner segments attached were also collected and analyzed using the same procedure. Finally, to provide controls for measurements of whole rods or isolated outer segments, 30-μl droplets of Ringer solution, or of Ringer solution containing known amounts of ATP or PCr, were deposited on a small plastic sheet and then treated in the same way as cell samples. The ATP and PCr content of the samples were assayed by the luciferin-luciferase luminescence method, following a procedure similar to that described by Lust et al. (1981). ATP was assayed first. For this, 250 μl of luciferin/luciferase buffer were introduced into a polystyrene test tube; 60 μl of sample were then added, and the luminescence produced was measured in a luminometer (LKB 1250). The luminescence produced by $<10^{-8}$ M ATP was low and somewhat noisy, but it decayed slowly (half-time was ~20 min). Therefore, to increase the accuracy of the measurement, the luminescence signal was recorded on chart paper for ~2 min and fitted with a straight line. The ATP signal was measured as the difference between the straight line extrapo-

lated back to the time of addition of the sample and the luminescence signal before addition of the sample. The assay was highly specific for ATP: the luminescence produced by GTP or ADP, at the same concentration as ATP, was >300 times less (i.e., less than the certified purity of the substances tested). Then, PCr was measured. This was done by measuring the extra ATP produced upon addition of creatine kinase to the test tube. For this, 15 μl of 10^{-5} M ADP solution was first added to the test tube. This caused a small increase of luminescence, and the new level of luminescence was recorded for ~30 s. Then, 15 μl of creatine kinase solution (5 U/μl) were added to the test tube. Typically, luminescence jumped immediately to a new level (this jump was due to the diadenosine phosphate that was added to the solution to inhibit myokinase activity); then it increased linearly for ~1 min and slowly curved for several minutes thereafter towards a maximum. [PCr] in the sample was proportional to the slope of the linear increase of luminescence. To increase the accuracy of the measurement, this linear portion of the recorded luminescence was fitted with a straight line, and the PCr signal was taken as the slope of this line. At intervals, during the assay procedure, ATP and PCr were measured in 60-μl samples of fresh ATP and PCr standards, to correct for any loss of enzyme activity (<10% after 2 h) in the reagents used. The ATP content of a sample of cells or of outer segments was determined by subtracting from the ATP signal in that sample, the ATP signal in samples of Ringer solution collected during the same experiment (which was typically <10% that in the cell sample), and by comparing this result with that obtained on the samples of ATP standards collected in that experiment. The same procedure was followed to determine the PCr content of these same samples.

Calculation of O_2 Consumption

The method used to calculate the rate of O_2 consumption of single rods was similar to that developed for the honeybee drone retina (Tsacopoulos and Poitry, 1982).

First, a one-dimensional model describing the diffusion of O_2 in and around the cell was chosen. In this model, the cell was considered as a truncated cylinder fitting in a hollow cylinder, the pipette, impermeable to O_2. The assumptions of the model were: (1) O_2 is consumed only within one sector of the cell of thickness h (this sector represented the ellipsoid body, which was clearly discernible on the video monitor screen of the experimental set-up, so that its thickness and its distance from the tip of the PO_2 microelectrode were readily measurable); (2) the rate of O_2 consumption, QO_2, is the same throughout that sector and varies only with time; (3) the solubility, α, and the diffusion coefficient, D, of O_2 in the cell are the same as in Ringer solution; (4) supply of O_2 to the cell occurs by diffusion along the axis of the suction pipette, either from the bath or from the solution filling the pipette; (5) the PO_2 has the same value, P_∞, in the bulk of the bath as in the bulk of the solution filling the pipette; (6) at the level of the tip of the PO_2 microelectrode, the net diffusion flux of O_2 from the bath is proportional to the difference between the local PO_2, P, and the PO_2 in the bulk of the bath; mathematically, this can be written as: $\partial P/\partial z = -\gamma\,[P_\infty - P]$, at $z = 0$ (where z is the space coordinate directed towards the interior of the pipette, along its axis, and γ is a constant >0 that needs to be derived from the measurements); (f) in the same way, at the extremity of the cell facing the interior of the suction pipette, the net diffusion flux of O_2 from the solution filling the pipette is proportional to the difference between the local PO_2 and the PO_2 in the bulk of the solution; this can be written as: $\partial P/\partial z = \gamma\,[P_\infty - P]$, at $z = L$ (where L is the distance between the tip of the PO_2 microelectrode and the extremity of the cell facing the interior of the pipette, and the constant γ is assumed to have the same value as above); (7) there is no discontinuity in the PO_2 and in the flux of O_2, which implies that P and $\partial P/\partial z$ are continuous functions of z, for $0 < z < L$. Then, the diffusion equation corresponding to this model was solved, both for steady state and for time-dependent conditions.

In steady-state conditions, the solution of the diffusion equation leads to the following relation (see APPENDIX):

$$Q_0 = \frac{\alpha D\gamma\,(2+\gamma L)\,(P_\infty - P_m)}{h\,\{1+\gamma\,[L-d]\}}, \qquad (1)$$

where Q_0 is the rate of O_2 consumption in the ellipsoid body in steady state (i.e., in darkness, in our experiments), d is the measured distance between the tip of the PO_2 electrode and the center of the ellipsoid body, P_m is the PO_2 measured by the electrode, and the other symbols are as defined above. There are only two unknowns, Q_0 and γ, in Eq. 1; all the other parameters are either known or were measured.

For time-dependent conditions, we solved the diffusion equation by the method of Fourier transforms (see e.g., Mahler, 1978). According to this method, if the rate of O_2 consumption departs only transiently from its steady-state value, the time course of this departure is related to the measured change of PO_2 by the following general equation:

$$\Delta Q(t) = \mathcal{F}_\omega^{-1}\{H[\omega]\,\mathcal{F}_t[\Delta P_m(t)]\}, \qquad (2)$$

where $\Delta Q(t)$ is the time course of the departure of Q from its steady-state value Q_o; $\mathcal{F}_t(.)$ denotes the Fourier transform, relative to t, of the function included in the brackets; $\mathcal{F}_\omega^{-1}(.)$ denotes the inverse Fourier transform; ω is the frequency conjugate to t; $\Delta P_m(t)$ is the time course of the PO_2 change measured by the electrode; and $H(\omega)$ is the transfer function of the problem at hand. In the particular case examined here, we found for the transfer function the following expression:

$$H(\omega) = A/[B-C], \qquad (3)$$

where: $A = \alpha D\mu\,\{(\mu^2+\gamma^2)\tanh(\mu L) + 2\mu\gamma\}$; $B = 2\sinh(\mu h/2)\sinh(\mu d)\,[\mu\tanh(\mu L)+\gamma]$; $C = 2\sinh(\mu h/2)\cosh(\mu d)\,[\mu+\gamma\tanh(\mu L)]$; $\mu = \sqrt{(i\omega/D)}$; [i is the imaginary number $\sqrt{-1}$, and sinh, cosh, and tanh denote the hyperbolic functions].

The procedure to compute the QO_2 of an isolated rod and to test the validity of the model was then as follows. First, we calculated the value of γ. For this, we assumed that the position of the cell relative to the PO_2 electrode does not affect the QO_2 in steady state. Therefore, using Eq. 1, we looked for the value of γ for which the values P_m measured at two different distances d from the ellipsoid body of the cell gave identical results for Q_o (see Results). Once the value of γ was determined, we then used Eqs. 2 and 3 to calculate the time course of the change of QO_2, $\Delta Q(t)$, corresponding to the PO_2 response, $\Delta P_m(t)$, recorded at either one of the two different sites. Numerical calculations and data acquisition were performed via the ASYST computer program (Asyst Software Technologies, Rochester, NY).

RESULTS

Light-induced PO_2 Response of Rod Photoreceptors

The experiments shown in Fig. 1 illustrate measurements made simultaneously of light-induced changes in transmembrane current and oxygen tension (PO_2) in the vicinity of an isolated rod photoreceptor. As illustrated schematically in Fig. 1 *a*, an isolated rod was drawn, outer segment first, into a glass recording pi-

pette connected to the current amplifier; the oxygen-sensitive microelectrode is shown approaching the rod inner segment from the right. Fig. 1 *c* shows that during a 3-min period of moderately bright light stimulation consisting of 90 flashes, 20 ms in duration, given every 2 s, over 90 percent of the rod's standing dark current was suppressed. During this same period, illustrated in Fig. 1 *e*, a biphasic change in the oxygen tension was measured; first there was a transient decrease in PO_2 followed by an increase which lasted until the termination of illumination, after which the PO_2 returned to baseline in darkness within ~5 min. In 66 experiments of the type illustrated in Fig. 1 *e*, the amplitude of the initial decrease of PO_2 ranged from <0.1 to ~0.5 mm Hg and that of the later increase of PO_2 ranged from 0.2 to 2 mm Hg. The same type of response is observed with continuous illumination, but this was not generally used because continuous light of an intensity sufficient to totally suppress the dark current caused substantial adaptative effects on the transmembrane photoresponse, which recovered slowly after termination of the light stimulus. This made the recovery of the PO_2 after this bright light difficult to interpret. The long stimulus consisting of many short bright flashes was adopted because it minimized the adaptative effects while producing a substantial, well defined, reduction in the dark current.

Since the change in the current measured by the O_2-sensitive microelectrode was typically <0.5 pA and since light causes a decrease of 20 pA or more in the dark current measured by the suction pipette, we devised two tests to ensure that the PO_2 signal truly reflected a change of PO_2 and was not some type of electrical artefact. The first of these tests is illustrated by a comparison of the results in the right and left panels of Fig.1. In this experiment, we compared for the same cell and the same light stimulus the effects on the PO_2 signal of reversing the direction of the transmembrane current relative to the current recording suction pipette. For this, we measured the light-induced change in PO_2 (ΔPO_2) and the rod electrical response with the cell drawn into the suction pipette as shown in Fig. 1 *a*. Then the cell was expelled from the suction pipette and reintroduced into the suction pipette, inner segment first (compare Fig. 1, *a* and *b*). In this configuration (Fig. 1 *b*), the dark current which is suppressed by light (Fig. 1 *d*) is flowing in the opposite direction inside the suction pipette and is opposite in sign to that shown in Fig. 1 *c*. However, the ΔPO_2 shown in Fig. 1 *e* is not reversed in sign compared to that shown in Fig. 1 *f*. Thus, this change in the orientation of the cell had no effect on the polarity and little effect on the amplitude of the ΔPO_2. This would be expected if the ΔPO_2 reflects a change in the rate of O_2 consumption of the cell, resulting from a light-induced change in oxygen

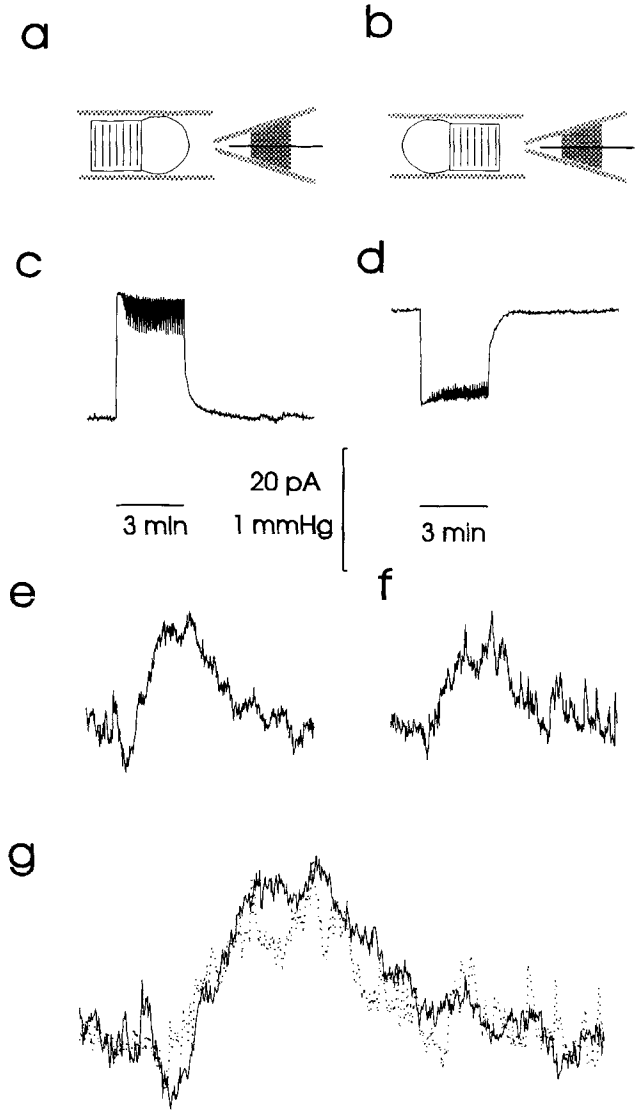

FIGURE 1. Simultaneous measurement of PO_2 and transmembrane current: effects of changing cell orientation. (*a* and *b*) Schematic of recording configuration: a rod photoreceptor is held inside a suction pipette with its outer segment (*striped*) pointing either inwards (*a*) or outwards (*b*); facing the opening of the suction pipette is the O_2-sensitive microelectrode. Diagram *a* describes the simultaneous recording of traces *c* and *e*, and diagram *b* describes traces *d* and *f*. (*c* and *d*) Light-induced transmembrane current responses recorded through the suction pipette (Note: the usual convention according to which current entering the cell is negative does not apply here: in order to make our point, the current in *d* is shown reversed, like it was in fact recorded by the suction pipette; thus, zero current corresponds to the uppermost part of the response in *c* and to the lowermost part of the response in *d*). (*e* and *f*) ΔPO_2 responses recorded by the O_2-sensitive microelectrode. (*g*) PO_2 traces *e* and *f* superimposed. The horizontal bars indicate both time scale and duration of stimulus for traces *c–f*; the vertical scale bar applies to traces *c–f*: the scale is 20 pA for traces *c* and *d*, and 1 mm Hg for traces *e* and *f*.

utilization, and is not the result of electrical interference between the suction pipette recording the transmembrane current and the electrode measuring the oxygen signal. This is best illustrated by comparison of the two ΔPO_2 responses in Fig. 1 *g*. Both are similar in time course and amplitude. Similar results were obtained in three other experiments of this type.

The tests illustrated in Fig.1 showed that the direction of the transmembrane current had no effect on the polarity and little effect on the amplitude of the ΔPO_2. However, this did not exclude the possibility that part of the response may be due to the light-induced increase in the electrical resistance between the interior of the suction pipette and the bath. This might be expected if the light-regulated membrane conductance could provide an alternative path for the current (~70 pA) resulting from the polarization of the O_2-sensitive microelectrode. To check that this was not the case, we constructed a suction pipette whose inner diameter was larger near its opening than 100 μm back from the tip (see diagrams in Fig. 2, *a* and *b*), and we measured the ΔPO_2 when the cell was held either close to the pipette's opening or at some distance back from the tip. Close to the pipette's opening, the cell fitted only loosely, because its diameter was significantly smaller than that of the pipette; therefore the increase in pipette resistance corresponding to the light response of the cell was small (Fig. 2 *c*). The ΔPO_2 recorded in this case is shown in Fig. 2 *e*. When the cell was drawn further into the interior of the pipette, it fitted tightly and the light-induced change in pipette resistance became much larger (see corresponding light response in Fig. 2 *d*). However, the ΔPO_2 recorded in this case was smaller, as we would expect since the cell was then more distant from the O_2-sensitive microelectrode. From the tests in Figs. 1 and 2 we conclude that the measured ΔPO_2 was unaffected by our recording of the light response of the cell.

Mitochondrial Origin of the ΔPO_2 Response

The ellipsoid body, which is the region of the inner segment adjacent to the outer segment, is packed with mitochondria (Townes-Anderson et al., 1985). To investigate whether the ΔPO_2 in Figs. 1 and 2 is mitochondrial in origin, we used Amytal, an inhibitor of mitochondrial respiration (see e.g., Slater, 1967). The experiment illustrated in Fig. 3 shows the membrane current and the PO_2 signal before and 25 min after exposure to 2 mM Amytal dissolved in the Ringer. This treatment resulted in about a 50% reduction in the dark current (Fig. 3 *b*) and an almost complete suppression of the ΔPO_2 (Fig. 3 *d*). For the purpose of comparison, the control ΔPO_2 and the response in Amytal are superimposed in Fig. 3 *e*. Similar results were obtained in eight

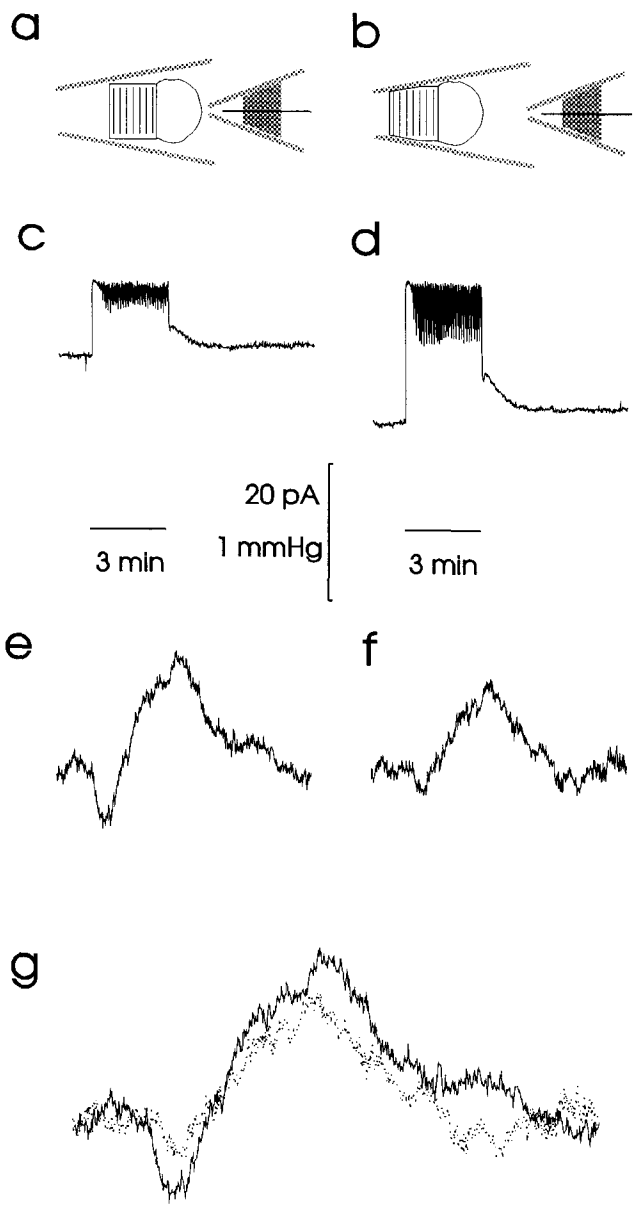

FIGURE 2. Simultaneous measurement of PO_2 and transmembrane current: effects of varying the electrical resistance of the seal around the cell. (*a* and *b*) Diagram describing the recording situation: the suction pipette is larger at its opening than further up, so that the cell fits in tightly only when it is sucked up into the pipette (*b*); diagram *a* describes the simultaneous recording of traces *c* and *e*, and diagram *b* describes traces *d* and *f*. (*c* and *d*) Light-induced transmembrane current responses; zero current corresponds to the top of each trace. (*e* and *f*) ΔPO_2 responses. (*g*) Traces *e* and *f* superimposed. The horizontal bars indicate both time scale and duration of stimulus for traces *c–f*; the vertical scale bar applies to traces *c–f*: the scale is 20 pA for traces *c* and *d*, and 1 mm Hg for traces *e* and *f*.

other cells. In seven of the nine cells tested, the effects of Amytal were completely reversible upon returning to normal Ringer; the two other cells did not recover. These results show that the PO_2 response reflects a

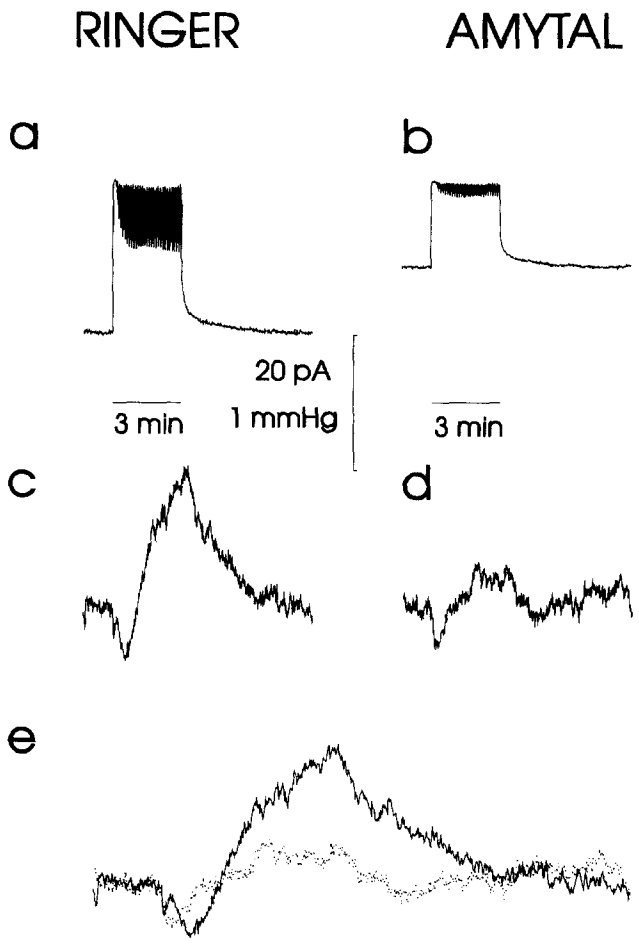

FIGURE 3. Suppression of the ΔPO_2 by the mitochondrial inhibitor Amytal. Traces *a* and *c* were recorded simultaneously in normal Ringer, and traces *b* and *d* were recorded simultaneously in Ringer containing 2 mM Amytal; cell orientation is that shown in Fig. 1 *a*. (*a* and *b*) Light-induced transmembrane current responses; the uppermost value in each trace corresponds to zero current. (*c* and *d*) ΔPO_2 responses. (*e*) traces *c* and *d* superimposed. The horizontal bars indicate both time scale and stimulus duration for traces *a–d*; the vertical scale bar applies to traces *a–d*: the scale is 20 pA for traces *a* and *b*, and 1 mm Hg for traces *c* and *d*.

change in mitochondrial respiration. However, by blocking mitochondrial respiration, Amytal probably reduced the concentration of ATP and therefore inhibited the transformation of GTP to cGMP. This may, in part, explain the reduction of the dark current. A number of experiments using different concentrations of Amytal were tested to see if a concentration could be found which would block respiration without affecting the dark current, but these were unsuccessful.

Dependence of the ΔPO_2 on Light Intensity

The typical ΔPO_2 at saturating light intensity (Fig. 3 *c*) consists of a slight decrease of PO_2 that lasts for ~1 min, followed by a larger increase of PO_2 that lasts for a few seconds after the end of stimulation and then returns slowly to baseline in ~5 min. This general shape varied however with the intensity of the stimulus. Fig. 4, *a–d* shows a sequence of light responses (*left column*) and the concomitant ΔPO_2 responses (*right column*) recorded on the same cell, for stimuli of different intensities. At low intensity (Fig. 4 *a*), only the rising phase of the ΔPO_2 was observed. As light intensity increased (traces *b*, *c*, and *d*), the amplitude of this rising phase increased, and the initial falling phase appeared gradually. To illustrate these differences in amplitude and time course more clearly, the ΔPO_2 responses in Fig. 4, *a* and *d* are also shown superimposed (Fig. 4 *e*).

To examine further how the ΔPO_2 relates to the electrical response of the cell, we compared in five cells the amplitude of the ΔPO_2 at the end of the stimulation period with the amplitude of the electrical response, for various light intensities. As an index of the amplitude of the electrical response, we chose the minimum value of the dark current suppression elicited by the stimulation (a value analogous to the plateau of the response obtained for a step stimulation), and expressed it as a percent of the maximum suppressible current for the cell considered. The results (Fig. 4 *f*) show that the ΔPO_2 increases over the same range of intensities as the plateau of the electrical response and that it increases in proportion with the amplitude of this plateau. This indicates a clear relationship between the suppression of the dark current and the increase of PO_2. Since the light response causes a decrease in the influx of both Na^+ and Ca^{2+} into rod photoreceptors, this relationship may result either from a decrease in the rate of ATP utilization by the Na-K-ATPase, or from a decrease in cytosolic $[Ca^{2+}]$ (see DISCUSSION).

Calculation of the Rate of Oxygen Consumption

To quantitate the rate of O_2 consumption (QO_2) of salamander rods and the change of QO_2 (ΔQO_2) reflected by their ΔPO_2 response, we made a model describing the diffusion of O_2 in and around the cell held in the pipette (see MATERIALS AND METHODS). To test whether this model gave an accurate description of O_2 diffusion in our experiments, we used recordings of the kind shown in Fig. 2 (traces *e* and *f*) which were obtained, for a given stimulus, with the cell positioned close to the O_2-sensitive microelectrode, and then farther from it. Since we knew the baseline value of the PO_2 measured by the O_2-sensitive microelectrode in those two situations (respectively 144.6 and 145.1 mm Hg, while the PO_2 in the bath was 147 mm Hg), we were able to calculate Q_o, the basal QO_2 of the cell, and the value of the parameter γ which determined the

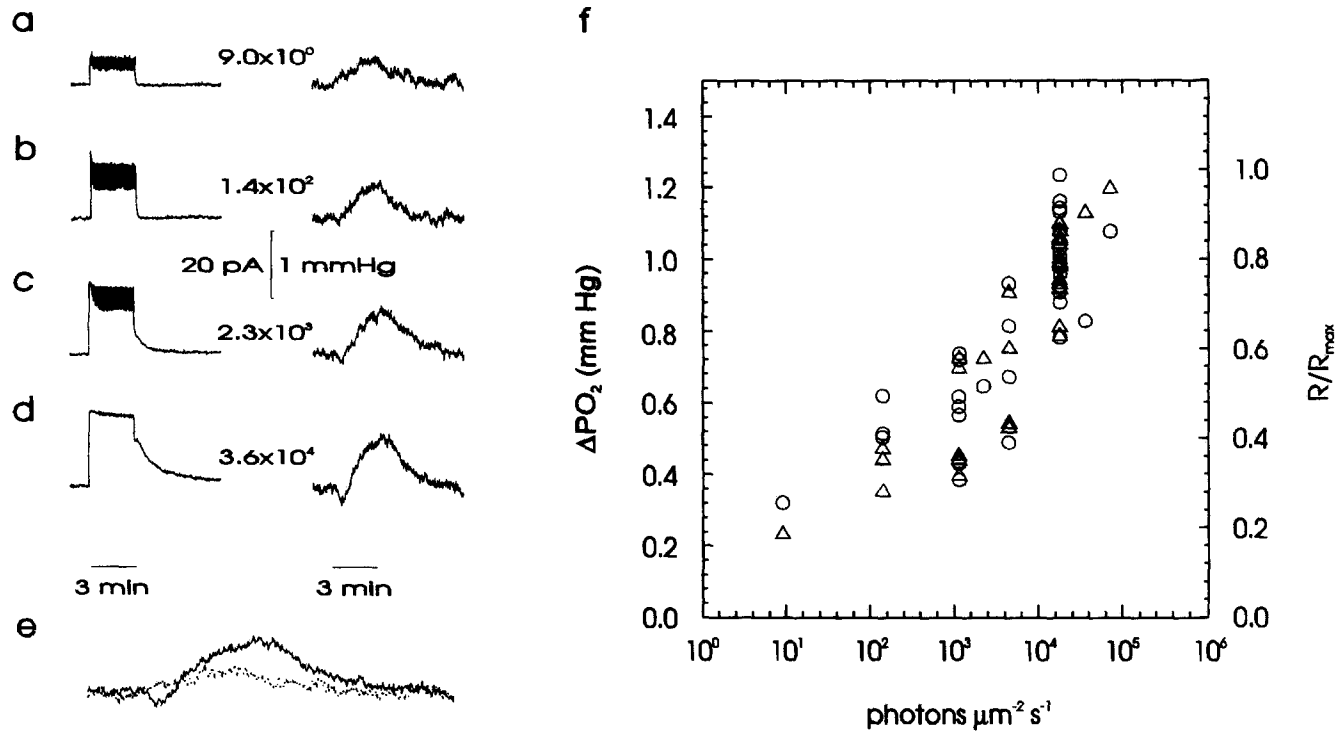

FIGURE 4. Dependence of transmembrane current and ΔPO_2 responses on light intensity. (*a–d*) Pairs of simultaneously recorded responses; the light-induced transmembrane current response is shown on the left, and the ΔPO_2 on the right. For each pair of responses, numbers give the intensity of the stimulus, expressed as number of photons per square micron and per s. The horizontal bars indicate both time scale and stimulus duration; the vertical scale bar is 20 pA for current responses and 1 mm Hg for ΔPO_2 responses. (*e*) PO_2 traces from *a* and *d* superimposed. (*f*) Comparison of the amplitudes of the plateau current suppression and of the ΔPO_2 for various light intensities; the data were obtained from pairs of light-induced transmembrane current (*triangles*) and ΔPO_2 responses (*circles*) collected on five cells; each cell contributed pairs of responses to light stimuli of at least three different intensities. The amplitude of ΔPO_2 responses was measured as the difference between the PO_2 3 min after the onset of stimulation and the PO_2 before stimulation. For the plateau current, the amplitude is expressed as the ratio of the minimum current suppression (R) induced by the stimulus, to the maximum suppressible current (R_{max}).

boundary conditions in our model (see Eq. 1, MATERIALS AND METHODS). The value that we obtained for the basal QO_2 was 24.7 μl O_2(STP) per ml of photoreceptor and per minute. Knowing the value of γ, we then calculated the time course of the light-induced ΔQO_2, using either the ΔPO_2 recorded close to the cell (which was the largest) or that recorded farther from it; since the ΔPO_2 responses were recorded for identical stimulations, the ΔQO_2 calculated from each response should match, if the model takes correctly into account the effects of diffusion. As shown in Fig. 5 *a*, this is indeed the case: both responses translated to a ΔQO_2 that decreases down to about −6 μl O_2(STP) per ml of photoreceptor and per min. From these data, the overall change of oxygen consumption induced by light can be calculated by simply adding one of the ΔQO_2 traces to the basal QO_2, and the result of this is presented in Fig. 5 *b*. Thus, we can conclude from these calculations that stimulation of salamander rod photoreceptors with moderately intense light causes the QO_2 to increase initially by ~10% and then subsequently decrease by ~25%.

Changes in ATP and Phosphocreatine Elicited by Light

To see whether the light-induced ΔQO_2 was controlled by ADP, we measured the levels of ATP and PCr under the same conditions as the physiological experiments just described (see Materials and Methods). The rationale was as follows: vertebrate photoreceptors contain PCr, in larger amounts than ATP (de Azeredo et al., 1981; Schnetkamp, 1986), and creatine kinase (Wallimann et al., 1986; Hemmer et al., 1993), the enzyme catalyzing the transfer of P_i from PCr to ADP or from ATP to creatine; therefore, any change in the rate of ATP utilization will affect not only [ATP], but also [PCr] (see e.g., Mahler, 1985; Chance et al., 1988). Moreover, since cytosolic creatine kinase functions primarily to maintain a low concentration of ADP (Lawson and Veech, 1979; Matthews et al., 1982), transient

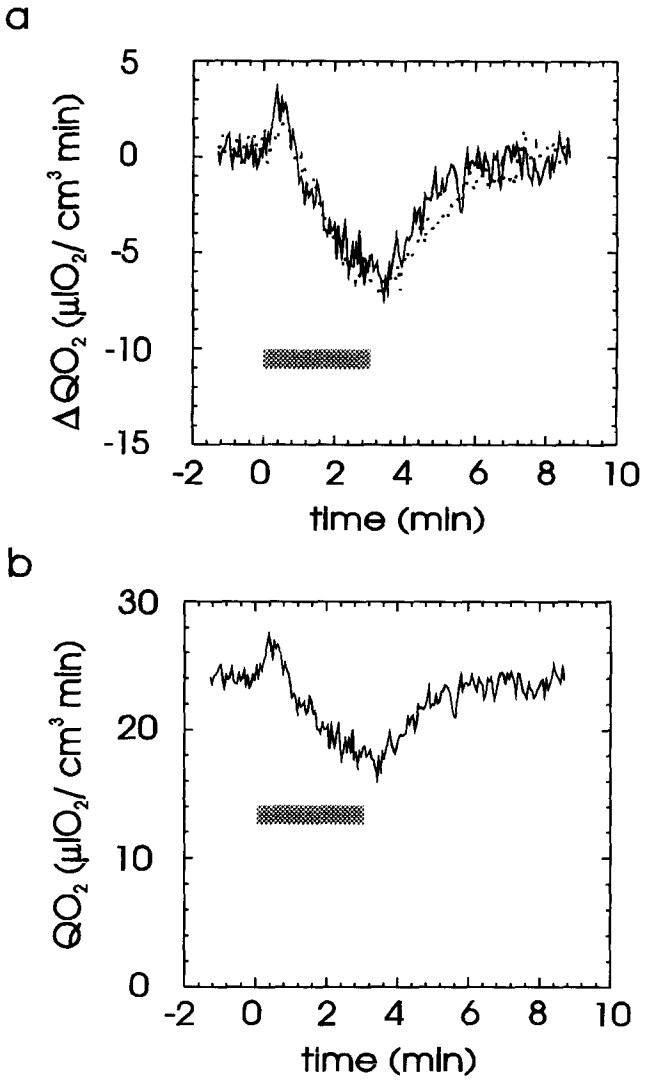

FIGURE 5. Change of O_2 consumption (ΔQO_2) induced by a stimulus of moderate intensity. (*a*) Comparison of the ΔQO_2 calculated from ΔPO_2 responses recorded either 43 (*solid trace*) or 15 μm (*dotted trace*) away from the cell (see diagrams in Fig. 2, *a* and *b*), for a fixed stimulus; the calculation was done using Eqs. 2 and 3, with $\gamma = 0.054\ \mu m^{-1}$. (*b*) Overall change of O_2 consumption; this trace was obtained by adding to the solid trace in *a* the value calculated for the resting O_2 consumption, using Eq. 1. Zero time corresponds to the onset of stimulation, and the shaded rectangle indicates the period of stimulation.

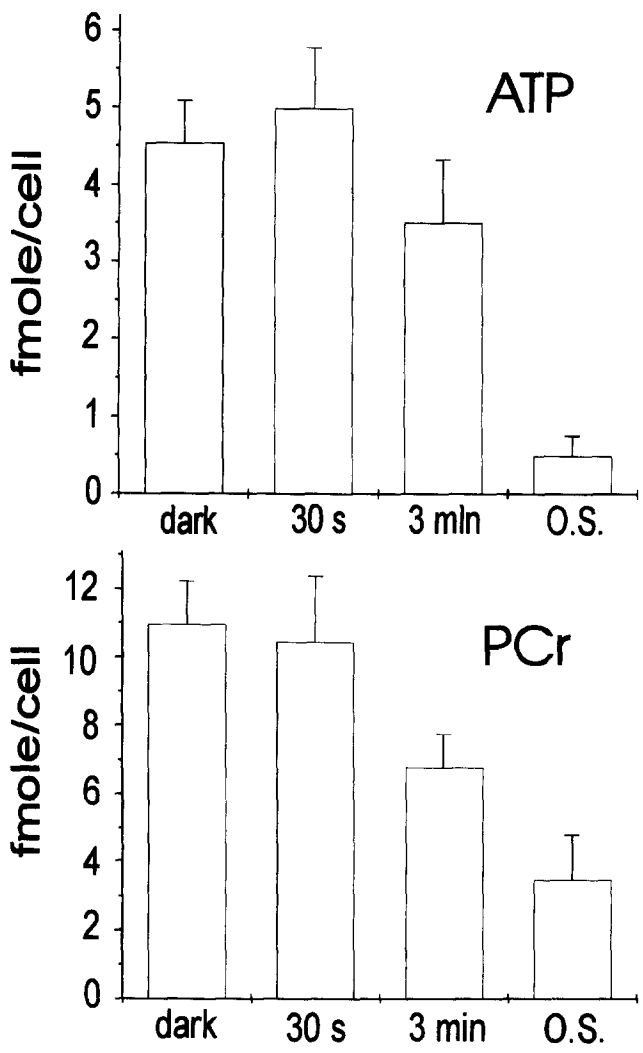

FIGURE 6. Amount of ATP and PCr in photoreceptors under various conditions, and in dark-adapted outer segments. For these experiments, samples containing from 27 to 71 photoreceptors were either kept 3 min in darkness (*dark*) or stimulated with 100-ms flashes of moderate intensity for 30 s or 3 min; for comparison, samples containing from 30 to 55 outer segments maintained in darkness (*O.S.*) were also collected. Results are expressed as amount per cell, and plotted values are mean ± SEM (*dark*: $n = 13$; *30 s*: $n = 6$; *3 min*: $n = 6$; *O.S.*: $n = 3$).

changes in the rate of ATP utilization are expected to cause much larger absolute changes in [PCr] than in [ATP] or [ADP]. Thus, our PCr measurements can be thought of as a surrogate for measurements of the cytosolic ADP levels which are too small to measure (see Chance et al., 1988): the concentration of PCr should increase (resp. decrease) when the level of ADP decreases (resp. increases). Therefore, if the ΔQO_2 was controlled by the level of cytosolic ADP, we would expect that at 30 s of illumination, when the QO_2 rises above the dark level, [PCr] should fall, and at 3 min of illumination, when the QO_2 falls below the dark level, [PCr] should rise.

In Fig. 6, we show measurements of ATP and PCr in the dark, and at 30 s and 3 min of illumination with 100-ms flashes of a light intensity (4×10^4 photons $\mu m^{-2}\ s^{-1}$) which maximally suppresses the dark current (see Fig. 4 *f*). At 30 s of illumination, there was no significant change in the levels of either ATP or PCr; however, a small decrease of 10% in PCr would be undetectable. At 3 min of illumination, there was no significant change in ATP and a 40% decrease in PCr. This change in PCr is exactly opposite to what we would pre-

dict (see above) if ADP levels were the controlling factor for mitochondrial respiration in the rods at 3 min of illumination.

DISCUSSION

We have developed a novel method for measuring light-induced changes in the oxygen consumption of single freshly isolated rod photoreceptors using miniature recessed-tip platinum oxygen electrodes. The method allows measuring very small changes in PO_2, typically less than 1% of the resting PO_2. Because the signals are so small, we carried out extensive control experiments (Figs. 1 and 2) to rule out the possibility that the measurements were confounded by subtle electrical artifacts. Taken together these control experiments indicate that illumination causes a biphasic change of PO_2: initially the PO_2 decreases during the first minute of illumination and then increases to a level above the resting value which is maintained until termination of illumination, after which the PO_2 returns to baseline in darkness over the subsequent 5 min. Using a one-dimensional model to describe the diffusion of O_2 in the cell and in the bathing solution, we calculate that the oxygen consumption (QO_2) of rods in darkness is ~24 μl O_2(STP) $min^{-1}ml^{-1}$, and that it increases transiently by ≈10% and then decreases by ≈25% during light stimulation (Fig. 5).

The occurrence of this decrease was earlier suggested by measurements of PO_2 performed at different depths in the intact retina of the cat by Linsenmeier and his co-workers (Linsenmeier, 1986; Haugh et al., 1990; Linsenmeier and Braun, 1992). In their studies, they took advantage of the fact that the photoreceptor layer is not vascularized, and they calculated the QO_2 of the photoreceptors by fitting the measured PO_2 to a mathematical model of diffusion. In darkness, their results were consistent with a QO_2 of 44–51 μl O_2(STP) $min^{-1}ml^{-1}$ in the photoreceptor layer at 37°C; when corrected for the temperature difference, these values are only ~20% less than the value we obtained. Under continuous illumination, the PO_2 profiles they measured differed in a way indicating a light-induced decrease of ~40% in the QO_2 of the photoreceptor layer. In a more recent study (Ahmed et al., 1993), using the same method on the macaque retina, they found similar values for the QO_2 in the photoreceptor layer. In addition, in the foveal region (which is avascular and cone rich), they measured a light-induced biphasic change of PO_2 that is similar to what we found for a single rod, if one takes into account the differences in temperature and cellular volume. Thus, the results of these studies are consistent with ours, and they indicate that under normal physiological conditions the QO_2 of photoreceptors is decreased by illumination, in the steady state.

The advantage of working on isolated rods is that the results are unambiguous and that it is possible to explore in more detail the mechanisms underlying the light-induced decrease of QO_2. This we did by comparing the intensity dependence for the suppression of the dark current with the intensity dependence for the increase of PO_2. The close correlation we found is consistent with the hypothesis that the decrease in QO_2 is caused by a light-induced decrease in the metabolic requirements of maintaining the photoreceptor dark current. This hypothesis is further supported by a quantitative estimate of the metabolic requirements of Na^+ pumping in darkness. The transmembrane current suppressed by light is about 40 pA. Since this current is carried essentially by Na^+ ions, it corresponds to the influx of about 2.4×10^{-14} moles of Na^+ per min. Taking that the volume of a rod is ~4×10^{-9} ml and that the theoretical stoichiometry $O_2/ATP/Na^+$ is 1:6:18 (see e.g., Stryer, 1988), the working of the Na-K-ATPase to extrude the excess Na^+ ions out of the rod would require the consumption of about 9 μl O_2(STP) $min^{-1}ml^{-1}$. This is more than one-third of the total QO_2 of a rod, and about this quantity was suppressed by light stimulation. However, this match should not be taken to indicate that the light-induced decrease in QO_2 is the direct result of the decrease in the intracellular concentration of Na^+ and of the consequent decrease in the hydrolysis of ATP by the Na-K-ATPase. The dark current is an inward current carried by both Na^+ and Ca^{2+}, and the plasma membrane of rods contains an Na^+/Ca^{2+} exchanger (Yau and Nakatani, 1984; Cervetto et al., 1989). Therefore, suppression of the dark current will cause a decrease in the intracellular concentrations of both Na^+ and Ca^{2+} (Na_i and Ca_i). Thus, either the decrease of Na_i or that of Ca_i might give rise to the decrease in QO_2.

The decrease in Na_i is expected to cause a decrease in the working of the Na-K-ATPase and thus an increase in the level of ATP and a decrease in the level of ADP. In addition, since photoreceptors possess a phosphocreatine buffering system (Hemmer et al., 1993), the decrease in ADP should be reflected as a large increase in PCr (see rationale in Results). Previous measurements of ATP and GTP levels in isolated rod photoreceptors are at odds with this expectation. Biernbaum and Bownds (1985) have shown that illumination causes a decrease in ATP and GTP levels, which would seem to indicate that metabolic requirements are increased by illumination rather than decreased. To resolve this apparent contradiction we measured the ATP and PCr levels in isolated rods under conditions that closely matched those of the physiological experiments. We found that ATP did not change significantly

under these conditions and PCr did not change after 30 s of illumination but decreased ~40% after 3 min of illumination (Fig. 6). To compare our measurements of ATP levels in isolated salamander rods with those of Biernbaum and Bownds (1985) in frog rods, we need to equate the light intensities in terms of pigment bleaching. Our measurements of the change in ATP level (Fig. 6) were done for a stimulus that resulted in a total bleach of 0.3%, which is in between the 0.003 and 2% bleaching stimuli they used (Fig. 4 of their study). In our study, the ATP levels after 30 s and 3 min were not significantly different from control, and in their study the ATP level transiently decreased on the order of 10–15% for both bleaches, taking longer to return to control for the larger bleach. However, our errors are such that a 10% change might have gone undetected. Our findings for ATP taken together with those of Biernbaum and Bownds (1985) are inconsistent with the idea, discussed above, that a light-induced decrease in Na_i causes an increase in the overall level of ATP and a concomitant decrease in ADP, with a consequent decrease in QO_2. Most importantly, our finding of a 40% decrease in PCr is precisely the opposite of what one would predict if the availability of ADP were regulating mitochondrial respiration.

The difficulty in interpreting this result however resides in that, due to the close packing of disks in the outer segment and to the cilium connecting inner and outer segments, the diffusion of metabolites between inner and outer segments is probably restricted. Thus, the light-induced decrease of Na^+ pumping may cause an increase of [PCr] in the inner segment while, in parallel, the light-induced increase in the rate of ATP utilization in the phototransduction machinery would cause [PCr] to decrease in the outer segment by a much larger amount than it increased in the inner segment. This would result in the overall decrease of [PCr] in the whole cell that we measured. While these effects have to be considered, it is difficult to strictly evaluate their importance in our results, since Townes-Anderson (1995) has found cytoplasmic bridges between inner and outer segments in about half of isolated rods from salamander. In addition, a restricted diffusion of nucleotides in the rod is difficult to conciliate with the initial transient rise of QO_2 (see below), since this rise would have then to reflect a light-induced increase in ATP utilization in the inner segment, which seems contradictory. Therefore, we do not think that the decreased activity of the Na-K-ATPase in the inner segment, with the corresponding decrease in ADP production, is the only mechanism contributing to the control of the QO_2 in rods.

The involvement of the working of the Na-K-ATPase in mediating light-induced changes in oxidative metabolism has been addressed previously in photoreceptors of invertebrates where, unlike in vertebrates, light causes an influx of Na^+ and a consequent rise in pumping activity. In honeybee drone photoreceptors (Tsacopoulos et al., 1983) and *Limulus* photoreceptors (Fein and Tsacopoulos, 1988*b*), activation of the Na-K-ATPase was not involved in the light-induced activation of O_2 consumption, whereas in barnacle photoreceptors the light-induced increase of oxygen consumption appeared to be caused by activation of sodium pumping and the consequent rise in ADP (Widmer et al., 1990).

The second candidate for causing the light-induced decrease in QO_2 is calcium. Indeed, Ca^{2+} in vitro stimulates respiration in mammalian mitochondria by activation of intramitochondrial dehydrogenases (for reviews, see Hansford, 1985; Denton and McCormack, 1990; McCormack and Denton, 1993, 1994), and it has been shown that light stimulation of the rod causes a decrease in Ca_i (see e.g., Kaupp and Koch, 1992) from ~300 nM to ~100 nM, i.e., in the range of concentration that may bring deactivation of mitochondrial enzymes (see e.g., Denton and McCormack, 1990; but compare to Medrano and Fox, 1994). How this might work is illustrated schematically in Fig. 7, where a light-induced decrease in Ca^{2+} influx results in a decrease of Ca_i in the outer segment, which will be reflected as a decrease of Ca_i in the inner segment as Ca^{2+} diffuses down its concentration gradient from the inner to the outer segment. The involvement of Ca_i in mediating changes in oxidative metabolism has been addressed previously in *Limulus* photoreceptors where light

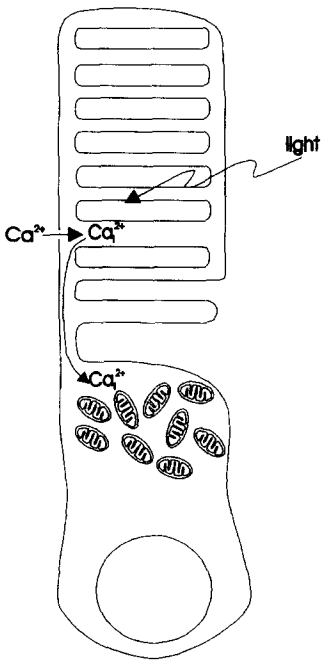

FIGURE 7. Ca^{2+} as possible link between the electrical response and the PO_2 response of photoreceptors. In darkness, Ca^{2+} enters the cell through the light-modulated channels and is extruded through the activity of the Na^+/Ca^{2+} exchanger (not shown). Cytosolic [Ca^{2+}] (Ca_i) is elevated in darkness thereby stimulating mitochondrial respiration. Light stimulation, by closing channels, causes the calcium influx to decrease and the continued action of the exchanger causes Ca_i to decrease, which in turn decreases respiration.

causes a rise in Ca_i. In *Limulus* photoreceptors oxidative metabolism is activated by Ca^{2+} (Fein and Tsacopoulos, 1988*a*).

Whether the light-induced decrease of QO_2 in rods is caused by a decrease of the local ADP level or of Ca_i, the measured decrease of [PCr] in the whole cell indicates that the rate of ATP hydrolysis did not decrease in parallel with the QO_2. Since such a mismatch between QO_2 and energy requirements of the cell would ultimately lead to depletion of ATP, there ought to be some control of the QO_2 by the nucleotide levels in the whole cell, on a larger time scale. In this respect, it is worth noting that, as reported by de Azeredo et al. (1981), [PCr] in the outer segment layer of the retina is decreased after 2 min illumination but is increased above its level in darkness after 2 h illumination.

The small transient increase of QO_2 occurring at the onset of photostimulation (see e.g., Fig. 3 *c*) may also reflect some control of QO_2 by nucleotides. Phototransduction is turned on immediately upon photostimulation, and, therefore, it precedes by far the decrease of Ca_i resulting from the combined work of the Na-K-ATPase and of the Na^+/Ca^{2+} exchanger (Ratto et al., 1988). It is possible that when Ca_i is relatively high, like in rod photoreceptors in darkness, mitochondrial enzymes are sufficiently activated that increases in the cytosolic level of ADP can cause an increase of QO_2. Thus, in a dark-adapted rod, the massive transformation of visual pigment elicited by intense light could induce a rapid rise in nucleotide turnover resulting in a small change in nucleotide levels (undetectable by our measurements), which in turn would cause an increase of QO_2. This small increase was only transient perhaps because of the later occurring decrease of Ca_i. Such a dual control of QO_2 by Ca_i and nucleotides may provide a subtle and quite efficient regulation for a mechanism as fundamental as the production of energy for cellular work.

APPENDIX

The one-dimensional diffusion equation corresponding to our model is:

$$\frac{\partial P(z,t)}{\partial t} = \frac{\partial^2 P(z,t)}{\partial z^2} - \frac{Q(z,t)}{\alpha D} \qquad \text{(A1)}$$

where $P(z,t)$ and $Q(z,t)$ are the time-dependent spatial distributions of PO_2 and QO_2, respectively; the other symbols are as defined in the text.

In this model, the system studied consisted of 3 contiguous regions of space: one extending from the tip of the PO_2 microelectrode ($z = 0$) to the ellipsoid body $z = \left(d - \frac{h}{2}\right)$, the second extending over the whole ellipsoid body, and the third from the ellipsoid body $z = d + \frac{h}{2}$ to the extremity of the cell facing the interior of the suction pipette ($z = L$). Furthermore, we assumed (assumptions 1 and 2 of the text) that $Q(z,t)$ could be written simply as:

$$Q(z,t) = \begin{cases} Q_0 + \Delta Q(t), & \text{for } d - \frac{h}{2} \le z \le d + \frac{h}{2} \\ 0, & \text{otherwise.} \end{cases} \qquad \text{(A2)}$$

In the steady state, when $\frac{\partial P(z,t)}{\partial t} = 0$ and $\Delta Q(t) = 0$, we have $Q(z,t) = Q_0$ and $P(z,t) = P(z)$. Under these conditions the solutions $P_j(z)$ (where $j = 1$, 2, or 3) to Eq. A1 in the three regions are (see for example Haugh et al., 1990):

$$\text{for } 0 \le z \le d - \frac{h}{2}: \quad P_1(z) = A_1 z + B_1 \qquad \text{(A3)}$$

$$\text{for } d - \frac{h}{2} \le z \le d + \frac{h}{2}: \quad P_2(z) = \frac{Q_0}{2\alpha D} z^2 + A_2 z + B_2 \qquad \text{(A4)}$$

$$\text{for } d + \frac{h}{2} \le z \le L: \quad P_3(z) = A_3 z + B_3 , \qquad \text{(A5)}$$

where A_1, B_1, A_2, B_2, A_3, and B_3 are arbitrary coefficients that are determined by the boundary conditions of the problem. The six boundary conditions were:

1) at $z = 0$ (assumption 6 of text):

$$A_1 = -\gamma [P_\infty - B_1] \qquad \text{(A6)}$$

2) continuity of P at $z = d - \frac{h}{2}$ (assumption 8 of text):

$$A_1\left[d - \frac{h}{2}\right] + B_1 = \frac{Q_0}{2\alpha D}\left[d - \frac{h}{2}\right]^2 + A_2\left[d - \frac{h}{2}\right] + B_2 \qquad \text{(A7)}$$

3) continuity of $\frac{dP}{dz}$ at $z = d - \frac{h}{2}$ (assumptions 3 and 8 of text):

$$\left(A_1 = \frac{Q_0}{\alpha D}\left[d - \frac{h}{2}\right] + A_2\right) \qquad \text{(A8)}$$

4) continuity of P at $z = d + \frac{h}{2}$ (assumption 8 of text):

$$\frac{Q_0}{2\alpha D}\left[d + \frac{h}{2}\right]^2 + A_2\left[d + \frac{h}{2}\right] + B_2 = A_3\left[d + \frac{h}{2}\right] + B_3 \qquad \text{(A9)}$$

5) continuity of $\frac{dP}{dz}$ at $z = d + \frac{h}{2}$ (assumptions 3 and 8 of text):

$$\frac{Q_0}{\alpha D}\left[d + \frac{h}{2}\right] + A_2 = A_3 \qquad \text{(A10)}$$

6) at $z = L$ (assumption 7 of text):

$$A_3 = \gamma [P_\infty - A_3 L - B_3] \ . \qquad \text{(A11)}$$

This system of equations can be rewritten as:

$$\begin{pmatrix} 1 & -\gamma & 0 & 0 & 0 & 0 \\ \left[d-\frac{h}{2}\right] & 1 & -\left[d-\frac{h}{2}\right] & -1 & 0 & 0 \\ 1 & 0 & -1 & 0 & 0 & 0 \\ 0 & 0 & -\left[d+\frac{h}{2}\right] & -1 & \left[d+\frac{h}{2}\right] & 1 \\ 0 & 0 & -1 & 0 & 1 & 0 \\ 0 & 0 & 0 & 0 & [1+\gamma L] & \gamma \end{pmatrix} \begin{pmatrix} A_1 \\ B_1 \\ A_2 \\ B_2 \\ A_3 \\ B_3 \end{pmatrix} = \begin{pmatrix} -\gamma P_\infty \\ \frac{Q_0}{2\alpha D}\left[d-\frac{h}{2}\right]^2 \\ \frac{Q_0}{\alpha D}\left[d-\frac{h}{2}\right] \\ \frac{Q_0}{2\alpha D}\left[d+\frac{h}{2}\right]^2 \\ \frac{Q_0}{\alpha D}\left[d+\frac{h}{2}\right] \\ \gamma P_\infty \end{pmatrix}. \quad \text{(A12)}$$

The values of all the parameters in these equations were known either through the assumptions made (for P_∞, α, and D) or through direct measurement (for h, d, and L), except for Q_0 and γ. We needed therefore two more conditions to completely determine the solution of the problem and to evaluate Q_0. One condition was provided by the measurement of PO_2: as the position of the tip of the PO_2 microelectrode was chosen as the origin of the spatial coordinate z, the measured PO_2, P_m, was equal to the coefficient B_1. Thus, solving the system of Eq. A12 for B_1, we obtained:

$$P_m = B_1 = \frac{\frac{Q_0}{\alpha D} h \{\gamma d - [1+\gamma L]\} + \gamma P_\infty [2+\gamma L]}{\gamma [2+\gamma L]}, \quad \text{(A13)}$$

which can be rewritten to yield Eq. 1 of the text. As for the second condition, it was obtained by measuring the PO_2 with the cell positioned close to the PO_2 microelectrode or away from it (see text).

To solve the time-dependent diffusion equation and to derive text Eq. 3, we used the method of Fourier transforms (see for example Mahler, 1978) and the same conditions as described above.

This work was supported by Swiss NSF grants 31-30038.90 and 31-37587.93, by the Kernen Foundation, and by National Institutes of Health grants EY01157 and EY03793.

Original version received 9 November 1995 and accepted version received 17 April 1996.

REFERENCES

Ahmed, J., R.D. Braun, R. Dunn, Jr., and R.A. Linsenmeier. 1993. Oxygen distribution in the macaque retina. *Invest. Ophthalmol. & Visual Sci.* 34:516–521.

Ames, A., Y.-Y. Li, E.C. Heher, and C.R. Kimble. 1992. Energy metabolism of rabbit retina as related to function: high cost of Na^+ transport. *J. Neurosc.* 12:840–853.

Biernbaum, M.S., and M.D. Bownds. 1985. Light-induced changes in GTP and ATP in frog rod photoreceptors. Comparison with recovery of dark current and light sensitivity during dark adaptation. *J. Gen. Physiol.* 85:107–121.

Cervetto, L., L. Lagnado, R.J. Perry, D.W. Robinson, and P.A. McNaughton. 1989. Extrusion of calcium from rod outer segments is driven by both sodium and potassium gradients. *Nature (Lond.).* 337:740–743.

Chance, B., J.S. Leigh, Jr., A.C. McLaughlin, M. Schnall, and T. Sinnwell. 1988. Phosphorus-31 spectroscopy and imaging. *In* Magnetic Resonance Imaging, 2nd ed., vol. 2 (Physical Principles and Instrumentation). C.L. Partain, R.R. Price, J.A. Patton, M.V. Kulkami, and A.E. James, Jr., editors. W.B. Saunders Co., Philadelphia. 1501–1520.

Cornwall, M.C., A. Fein, and E.F. MacNichol, Jr. 1990. Cellular mechanisms that underlie bleaching and background adaptation. *J. Gen. Physiol.* 96:345–372.

Darnell, J.E., H.F. Lodish, and D. Baltimore. 1986. Molecular Cell Biology. Scientific American Books, New York. 890 pp.

de Azeredo, F.A.M., W.D. Lust, and J.V. Passonneau. 1981. Light-induced changes in energy metabolites, guanine nucleotides, and guanylate cyclase within frog retinal layers. *J. Biol. Chem.* 256: 2731–3735.

Denton, R.M., and J.G. McCormack. 1990. Ca^{2+} as a second messenger within mitochondria of the heart and other tissues. *Annu. Rev. Physiol.* 52:451–466.

Fein, A., and E.Z. Szuts. 1982. Photoreceptors: their role in vision. Cambridge University Press, Cambridge, U.K. 29–38.

Fein, A., and M. Tsacopoulos. 1988*a*. Activation of mitochondrial oxidative metabolism by calcium ions in *Limulus* ventral photoreceptor. *Nature (Lond.).* 331:437–440.

Fein, A., and M. Tsacopoulos. 1988*b*. Light-induced O_2 consumption in *Limulus* ventral photoreceptors does not result from a rise in intracellular sodium concentration. *J. Gen. Physiol.* 91:515–527.

Hansford, R.G. 1985. Relation between mitochondrial calcium transport and control of energy metabolism. *Rev. Physiol. Biochem. Pharmacol.* 102:1–72.

Haugh, L.M., R.A. Linsenmeier, and T.K. Goldstick. 1990. Mathe-

matical models of the spatial distribution of retinal oxygen tension and consumption, including changes upon illumination. *Ann. Biomed. Eng.* 18:19–36.

Hemmer, W., I. Riesinger, T. Wallimann, H.M. Eppenberger, and A.F.G. Quest. 1993. Brain-type creatine kinase in photoreceptor cell outer segments: role of a phosphocreatine circuit in outer segment energy metabolism and phototransduction. *J. Cell Sci.* 106:671–684.

Kaupp, U.B., and K.-W. Koch. 1992. Role of cGMP and Ca^{2+} in vertebrate photoreceptor excitation and adaptation. *Annu. Rev. Physiol.* 54:153–175.

Lawson, J.W.R., and R.L. Veech. 1979. Effects of pH and free Mg^{2+} on the K_{eq} of the creatine kinase reaction and other phosphate hydrolyses and phosphate transfer reactions. *J. Biol. Chem.* 254: 6528–6537.

Lehninger, A.L. 1982. Principles of Biochemistry. Worth Publishers, Inc., New York. 518, 536–540.

Linsenmeier, R.A. 1986. Effects of light and darkness on oxygen distribution and consumption of the intact cat retina. *J. Gen. Physiol.* 88:521–542.

Linsenmeier, R.A., and R.D. Braun. 1992. Oxygen distribution and consumption in the cat retina during normoxia and hypoxemia. *J. Gen. Physiol.* 99:177–197.

Lundin, A., M. Hasenson, J. Persson, and A. Pousette. 1986. Estimation of biomass in growing cell lines by adenosine triphosphate assay. *Methods Enzymol.* 133:27–42.

Lust, W.D., G.K. Feussner, E.K. Barbehenn, and J.V. Passonneau. 1981. The enzymatic measurement of adenine nucleotides and P-creatine in picomole amounts. *Anal. Biochem.* 110:258–266.

Mahler, M. 1978. Kinetics of oxygen consumption after a single isometric tetanus of frog sartorius muscle at 20°C. *J. Gen. Physiol.* 71: 559–589.

Mahler, M. 1985. First-order kinetics of muscle oxygen consumption, and an equivalent proportionality between QO_2 and phosphorylcreatine level. Implications for the control of respiration. *J. Gen. Physiol.* 86:135–165.

Matthews, P.M., J.L. Bland, D.G. Gadian, and G.K. Radda. 1982. A ^{31}P-NMR saturation transfer study of the regulation of creatine kinase in the rat heart. *Biochim. Biophys. Acta.* 721:312–320.

McCormack, J.G., and R.M. Denton. 1993. Mitochondrial Ca^{2+} transport and the role of intramitochondrial Ca^{2+} in the regulation of energy metabolism. *Dev. Neurosci.* 15:165–173.

McCormack, J.G., and R.M. Denton. 1994. Signal transduction by intramitochondrial Ca^{2+} in mammalian energy metabolism. *News Physiol. Sci.* 9:71–76.

Medrano, C.J., and D.A. Fox. 1994. Substrate-dependent effects of calcium on rat retinal mitochondrial respiration: physiological and toxicological studies. *Toxicol. Appl. Pharmacol.* 125:309–321.

Passonneau, J.V., and O.H. Lowry. 1993. Enzymatic Analysis: A Practical Guide. Humana Press, Totowa, NJ. 123 pp.

Ratto, G.M., R. Payne, W.G. Owen, and R.Y. Tsien. 1988. The concentration of cytosolic free calcium in vertebrate rod outer segments measured with fura-2. *J. Neurosci.* 8:3240–3246.

Schnetkamp, P.P.M. 1986. Sodium-calcium exchange in the outer segments of bovine rod photoreceptors. *J. Physiol.* 373:25–45.

Slater, E.C. 1967. Application of inhibitors and uncouplers for a study of oxidative phosphorylation. *Methods Enzymol.* 10:48–57.

Stryer, L. 1988. Biochemistry, 3rd ed. W.H. Freeman & Co, New York. 420, 421, 952.

Townes-Anderson, E. 1995. Intersegmental fusion in vertebrate rod photoreceptors. Rod cell structure revisited. *Invest. Ophthalmol. & Visual Sci.* 36:1918–1933.

Townes-Anderson, E., P.R. MacLeish, and E. Raviola. 1985. Rod cells dissociated from mature salamander retina: ultrastructure and uptake of horseradish peroxidase. *J. Cell Biol.* 100:175–188.

Tsacopoulos, M., and S. Poitry. 1982. Kinetics of oxygen consumption after a single flash of light in photoreceptors of the drone (*Apis mellifera*). *J. Gen. Physiol.* 80:19–55.

Tsacopoulos, M., S. Poitry, and A. Borsellino. 1981. Diffusion and consumption of oxygen in the superfused retina of the drone (*Apis mellifera*) in darkness. *J. Gen. Physiol.* 77:601–628.

Tsacopoulos, M., R.K. Orkand, J.A. Coles, S. Levy, and S. Poitry. 1983. Oxygen uptake occurs faster than sodium pumping in bee retina after a light flash. *Nature (Lond.).* 301:604–606.

Wallimann, T., G. Wegmann, H. Moser, R. Huber, and H.M. Eppenberger. 1986. High content of creatine kinase in chicken retina: compartmentalized location of creatine kinase isoenzymes in photoreceptor cells. *Proc. Natl. Acad. Sci. USA.* 83:3816–3819.

Widmer, H., S. Poitry, and M. Tsacopoulos. 1990. The increase of oxygen consumption after a flash of light is tightly coupled to sodium pumping in the lateral ocellus of barnacle. *J. Gen. Physiol.* 96:83–108.

Yau, K.-W., P.A. McNaughton, and A.L. Hodgkin. 1981. Effect of ions on the light-sensitive current in retinal rods. *Nature (Lond.).* 292:502–505.

Yau, K.-W., and K. Nakatani. 1984. Electrogenic Na-Ca exchange in retinal rod outer segment. *Nature (Lond.).* 311:661–663.